

# Magnetic Resonance Studies of Ammonia Adsorption and Decomposition on Titania-Supported Vanadia Catalysts

Marjorie S. Went<sup>†</sup> and Jeffrey A. Reimer\*

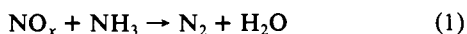
Contribution from the Center for Advanced Materials, Lawrence Berkeley Laboratory, and Department of Chemical Engineering, University of California at Berkeley, Berkeley, California 94720-9989. Received October 3, 1991

**Abstract:** In-situ proton and deuteron single-resonance NMR techniques were used to study the adsorption and decomposition of ammonia as a function of temperature on a series of V<sub>2</sub>O<sub>5</sub>/TiO<sub>2</sub> catalysts with the weight loading of vanadia ranging from 0 to 6.1 wt % (approximately one monolayer). After analysis of magnetic resonance line shapes, several different molecular species were found to be present on the catalyst surfaces. At low adsorption temperatures on the low-loading samples, the predominant adsorbed species was intact, coordinated ammonia rotating about its C<sub>3</sub> axis. As the weight loading or adsorption temperature was increased, the adsorbed, intact ammonia exhibited an increased H-N-H angle; the total number of protons associated with intact ammonia per gram of sample decreased. At the point where intact ammonia was no longer observed, a new species was observed and assigned to NH<sub>2</sub> moieties. On all samples, ammonium ions were observed at low adsorption temperatures (100 °C) but were found to be easily removed by heating. Their concentration was greater on the higher weight loading samples. The formation of short-lived VOH groups from the protons of dissociated NH<sub>3</sub> was inferred on the higher weight loading samples. Multiple-quantum spin-counting experiments were done to further investigate the nature of the adsorbed species and their groupings on the surfaces.

## Introduction

The elimination of anthropogenic sources of NO<sub>x</sub> is increasingly important as new air pollution standards are being implemented. NO<sub>x</sub> compounds exhibit deleterious effects on the environment, notably as reactants in photochemical smog and as precursors to the formation of "acid rain". Considerable attention has been focused on combustion modification techniques, which both reduce NO<sub>x</sub> emissions and are cost effective and energy efficient. These techniques, however, do not provide sufficient reduction to meet new and anticipated air quality standards. Noncatalytic methods for the chemical reduction of NO<sub>x</sub> compounds, such as homogeneous gas-phase processes which use ammonia as a reducing agent, require high operating temperatures and a high ammonia to NO<sub>x</sub> ratio. Chemical scrubbing of stack gases results in large concentrations of unwanted aqueous byproducts.

One method of choice for reduction of NO<sub>x</sub> emissions from fixed sources is selective catalytic reduction (SCR), with ammonia being the most selective reducing agent. The overall process may be written as



where the addition of O<sub>2</sub> to the reaction mixture enhances the activity. The SCR of NO<sub>x</sub> with ammonia has been the subject of extensive review.<sup>1</sup> Supported vanadia as a catalyst is effective, exhibits high activity over a wide range of modest operating temperatures (150–500 °C), is resistant to poisoning by sulfur oxides, and is inexpensive compared to supported metals such as platinum.

Optimum catalytic behavior is observed when vanadia is supported on the anatase phase of titania or on mixed titania/silica supports. On these catalysts the NO<sub>x</sub> conversion per surface vanadium atom reaches<sup>2–4</sup> a maximum at a surface coverage of about one molecular monolayer, for any given temperature. The selectivity toward nitrogen at maximum conversion temperature remains greater than 95% up to coverages of approximately one-half monolayer and then drastically decreases<sup>4,5</sup> as the weight loading is further increased.

The surface structure of supported vanadia catalysts has been studied by various spectroscopies, including vibrational,<sup>6,7</sup> EXAFS,<sup>8</sup> and magnetic resonance.<sup>8,9</sup> At very low loadings (less than 3 wt %), the predominant vanadia species are monomeric vanadyls.

As the loading is increased to about one monolayer (approximately 6 wt %), polymeric vanadyl species are present in increasing amounts. Above one monolayer, crystallites of V<sub>2</sub>O<sub>5</sub> form on the surface.

The vanadia and exposed titania surface sites exhibit both Bronsted and Lewis acidity toward ammonia adsorption. Lewis acid sites which coordinatively adsorb ammonia have been identified via infrared spectroscopy<sup>10–17</sup> on titania as well as on pure and supported vanadia. Some evidence indicates that the Lewis acid sites on the vanadia or on the titania-supported vanadia are stronger than those on pure titania; at elevated temperatures, ammonia tends to desorb from Lewis acid sites on the titania and readsorb on Lewis acid sites on the vanadia, resulting<sup>11,13</sup> in a high-frequency shift of the infrared band of the more strongly coordinated ammonia. Raman spectroscopy has shown<sup>18</sup> that the monomeric vanadyls on the surface of very low weight loading titania-supported vanadia samples are perturbed by ammonia adsorption at low temperatures, suggesting coordination to the V=O group. This perturbation is ameliorated as the temperature is increased and less ammonia interacts with the surface. On higher weight loading samples, the monomeric species are irreversibly perturbed,<sup>18</sup> indicating chemical reduction; polymeric

- (1) Bosch, H.; Janssen, F. *Catal. Today* **1988**, *2*, 369.
- (2) Bjorkland, R. B.; Odenbrand, C. U. I.; Brandin, J. G. M.; Andersson, L. A. H.; Liedberg, B. *J. Catal.* **1989**, *119*, 187.
- (3) Bosch, H.; Janssen, F. J. G.; van den Kerkhof, F. M. G.; Oldenzel, J.; van Ommen, J. G.; Ross, J. R. H. *Appl. Catal.* **1986**, *25*, 239.
- (4) Went, G. T.; Leu, L.-J.; Rosin, R. R.; Bell, A. T. *J. Catal.*, in press.
- (5) Vogt, E. T. C.; Boot, A.; van Dillen, A. J.; Geus, J. W.; Janssen, F. J. G.; van den Kerkhof, F. M. G. *J. Catal.* **1988**, *114*, 313.
- (6) Busca, G.; Centi, G.; Marchetti, L.; Trifiro, F. *Langmuir* **1986**, *2*, 568.
- (7) Oyama, S. T.; Went, G. T.; Lewis, K. B.; Bell, A. T.; Somorjai, G. A. *J. Phys. Chem.* **1989**, *93*, 6786.
- (8) Kozlowski, R.; Pettifer, R. F.; Thomas, J. M. *J. Phys. Chem.* **1983**, *87*, 5176.
- (9) Eckert, H.; Wachs, I. E. *J. Phys. Chem.* **1989**, *93*, 676.
- (10) Topsøe, N. *J. Catal.* **1991**, *128*, 128.
- (11) Ramis, G.; Busca, G.; Bregani, F.; Forzatti, P. *Appl. Catal.* **1990**, *64*, 259.
- (12) Rajadhyaksha, R. A.; Knozinger, H. *Appl. Catal.* **1989**, *51*, 81.
- (13) Busca, G. *Langmuir* **1986**, *2*, 577.
- (14) Busca, G.; Saussey, H.; Saur, O.; Lavalley, J. C.; Lorenzelli, V. *Appl. Catal.* **1985**, *14*, 245.
- (15) Miyata, H.; Nakagawa, Y.; Ono, T.; Kubokawa, Y. *Chem. Lett.* **1983**, 1141.
- (16) Inomata, M.; Mori, K.; Miyamoto, A.; Ui, T.; Murakami, Y. *J. Phys. Chem.* **1983**, *87*, 754.
- (17) Tsyganenko, A. A.; Pozdnyakov, D. V.; Filimonov, V. N. *J. Mol. Struct.* **1975**, *29*, 299.
- (18) Went, G. T.; Leu, L.-J.; Lombardo, S. J.; Bell, A. T. *J. Phys. Chem.*, in press.

\* To whom correspondence should be addressed at the Department of Chemical Engineering.

<sup>†</sup> Current address: Biotechnology Program, Cornell University, Ithaca, NY 14853.

species are also reduced by ammonia adsorption at higher temperatures.

Surface hydroxyl groups may act as Bronsted acid sites which react to form ammonium ions upon exposure to ammonia. Infrared spectroscopy studies have shown that those Bronsted acid sites which lead to the formation of ammonium ions exist on both vanadia and supported vanadia but not on pure titania of comparable surface areas. These hydroxyl sites show stronger<sup>10,13</sup> molecular adsorption energies on titania-supported vanadia than on vanadia alone. Several studies<sup>10,11,13</sup> have shown that, at temperatures of 250 °C or higher, equilibrium favors gas-phase ammonia. The proportion of Bronsted sites to Lewis sites has been found<sup>15,16,19</sup> to increase as the weight loading of vanadia on titania increases from 0 wt % to close to one monolayer.

Ammonia adsorption on titania-supported vanadia has also been studied<sup>18</sup> by temperature-programmed desorption (TPD). These data show that as vanadia weight loading is increased from 0 to 3 wt %, ammonia desorbs at progressively higher temperatures, suggesting increasing adsorption energies with weight loading. Higher weight loadings, e.g. 6 wt %, show qualitatively different behavior, with ammonia easily desorbing by 200 °C. The fraction of dissociated products,  $(\frac{1}{2}[\text{N}_2] + [\text{NO}_x])/[\text{NH}_3]_{\text{ads}}$ , as quantified with TPD, was found to increase monotonically with weight loading. Water desorbs from pure titania as one peak at a relatively high temperature of ~400 °C, but from the higher vanadia weight loading samples, water desorbs as several peaks. Dinitrogen desorption quantitatively increases and shifts to lower temperature as vanadia weight loading is increased. These TPD results will be interpreted further in the Discussion.

Nitrous oxides do not strongly interact<sup>1</sup> with these catalysts. The chemistry of ammonia adsorption, on the other hand, is clearly very complex. Elucidation of this chemistry on supported vanadia catalysts is a necessary first step toward an understanding of the mechanism of selective catalytic reduction. The goal of this study is to apply solid-state magnetic resonance techniques to achieve a molecular level understanding of the influence of vanadia surface structure on the adsorption and decomposition of ammonia. This is done by examining the proton and deuteron magnetic resonance spectra of ammonia molecules adsorbed at various temperatures on samples of titania-supported vanadia where the vanadia concentrations range from 0 wt % to greater than one monolayer. Four separate molecular structures are identified after ammonia adsorption on the catalyst surfaces. They are (i) intact, coordinated, and rapidly rotating ammonia molecules, (ii)  $\text{NH}_x$  decomposition products, (iii) ammonium ( $\text{NH}_4^+$ ) ions, and (iv) surface hydroxyl groups. The distribution of these structures as a function of both surface composition and adsorption temperature yields information regarding adsorption sites.

## Experimental Section

**Catalyst Preparation.** To prepare the titania (anatase) support, titanium isopropoxide (Du Pont Tylzar) was added dropwise at a rate of 1 mL/min to a mixture of distilled water and 2-propanol (Fisher Scientific Spectranalyzed, Class 1B), which was stirring in a salt and ice-water bath at  $-7 \pm 2$  °C, according to a method<sup>20</sup> applied previously. The solution containing fine particles of TiOH was decanted, and the particles were washed with distilled water, isolated by filtration in a Buchner funnel, and again washed. The resulting powder was dried in an oven overnight at 120 °C with a nitrogen purge and then dried under vacuum at 120 °C. It was then calcined in batches in 150 cm<sup>3</sup>/min of oxygen for 4–10 h at 200 °C followed by 6–13 h at 450 °C. The titania was characterized by X-ray diffraction and Raman spectroscopy and estimated to be >95% anatase phase with some brookite phase and no detectable rutile phase.

Supported vanadia catalysts were prepared using standard<sup>7</sup> incipient-wetness impregnation techniques. For each sample, the amount of ammonium metavanadate (Aldrich Gold Label, 99.99%) required to give the desired weight percent of  $\text{V}_2\text{O}_5$  was slowly added to a stoichiometric amount (2 equiv) of oxalic acid (anhydrous, Aldrich Gold Label, 99+%) partially dissolved in a small amount of distilled water while the mixture was being stirred and heated to approximately 80 °C until all solids were

Table I. Catalyst Characteristics

wt % vanadia	BET surface area <sup>b</sup> (m <sup>2</sup> /g)	color	
		oxidized	reduced in ammonia
0 (TiO <sub>2</sub> )	96.9	white	white
1.3	79.4	pale yellow	light green-gray
3.0	78.3	yellow	gray to blue-gray
6.1	44.0	orange-brown	gray to dark blue

<sup>a</sup> Determined by XRF to an accuracy of  $\pm 6\%$ . <sup>b</sup> Determined to an accuracy of  $\pm 10\%$ .

dissolved. The solution was then cooled to room temperature and diluted to the appropriate volume determined by the incipient-wetness point of the titania, 0.8–1.1 mL/g. This solution was added dropwise to the titania, and the resulting mixture was ground in a mortar and pestle slowly. The resulting brown paste was dried in an oven at 115 °C overnight. For the higher weight loadings (e.g. 6.1 wt %), two impregnations were performed with an intermediate drying period. The powder was pelletized (for positioning on quartz reactor frits in the characterization studies) to particles of diameter 250–600  $\mu\text{m}$  (30–60 mesh). It was then calcined in 150 cm<sup>3</sup>/min of oxygen for 3–4 h at 200 °C, followed by 4 h at 450–500 °C, and then cooled overnight in 50 cm<sup>3</sup>/min of oxygen. The oxidized samples ranged in color from pale yellow to orange-brown. Reduction with ammonia changed the colors to greenish gray to dark blue-gray.

Elemental analysis for impurities yielded <35 ppm of iron in all samples, <90 ppm of potassium in all samples, 130 ppm of sodium in the 1.3 wt % sample, and <80 ppm of sodium in the others. The weight loadings of vanadia were determined by X-ray fluorescence spectroscopy using the  $K\beta$  X-rays of vanadium and using titanium as an internal standard. The results are listed in Table I along with the BET surface areas as determined by  $\text{N}_2$  adsorption.

Previous work<sup>7,18</sup> on identical samples has established that, on the 1.3 wt % sample, monomeric vanadyl species dominate on the surface; on the 3.0 wt % sample, both monomeric and polymeric  $\text{VO}_x$  species are present; and on the 6.1 wt % sample, one monolayer of  $\text{VO}_x$  species covers the titania.

**Preparation of Samples for NMR.** One gram of the pelletized  $\text{V}_2\text{O}_5/\text{TiO}_2$  sample was loaded into a quartz microreactor, with the NMR coil wound around the sample volume, and sealed in the NMR probe with Cajon Ultratorr fittings. The probe was transported to a glass chemisorption rack for the adsorptions.  $\text{V}_2\text{O}_5/\text{TiO}_2$  was first calcined for 1 h at 510 °C in 60 cm<sup>3</sup>/min of flowing oxygen. The sample was cooled to the adsorption temperature or 250 °C, whichever was higher, in flowing oxygen. The flow was then switched to helium for  $\frac{1}{2}$  h at the same flow rate to purge residual oxygen from the system. If not there already, the sample was cooled to the adsorption temperature and then subjected to a mixture of 1.07% ammonia in helium flowing at 60 cm<sup>3</sup>/min for  $\frac{1}{2}$  h. Next, the sample was purged in 100 cm<sup>3</sup>/min of helium for 1 h, followed by rapid quenching to room temperature. The probe was sealed in slightly greater than 1 atm of helium and was then ready for the NMR experiments. Spectra taken of samples prepared this way yield spectral parameters that reflect the nature of the irreversibly adsorbed, stable species present on the surface at the adsorption temperature. It is worth noting that flowing adsorptions were chosen over static adsorptions for better duplication of the conditions of TPD and kinetic studies and for the practical advantage of reduced temperature gradients. Diffusion gradients were discovered, by virtue of the color change of vanadia upon reduction, to be significant. It was necessary to use a low flow rate and also to overpack the microreactor to avoid channeling.

Static adsorptions were done separately to obtain quantitative information on the ammonia uptakes. Figure 1 shows adsorption isotherms for  $\text{NH}_3$  on the 3.0 wt % sample at 100 and 400 °C. The total irreversible uptakes were 5.1 and 1.9  $\mu\text{mol}/\text{m}^2$ , respectively. It can be seen qualitatively that, of the total adsorption, a larger fraction is reversible (physisorption) at 400 °C.

**NMR Experiments.** Proton NMR spectra were obtained for  $\text{NH}_3$  adsorbed at temperatures of 100, 250, and 400 °C, with calcinations preceding each adsorption, on  $\text{TiO}_2$  and on 1.3, 3.0, and 6.1 wt %  $\text{V}_2\text{O}_5/\text{TiO}_2$ . Background spectra were also obtained for each of the freshly calcined samples. Proton multiple-quantum experiments were done for ammonia adsorbed at 100 °C on  $\text{TiO}_2$  and on 3.0 and 6.1 wt %  $\text{V}_2\text{O}_5/\text{TiO}_2$ .

The proton experiments were accomplished with a commercial (NCC Quest 4000) spectrometer operating at 400 MHz, using a home-built<sup>21</sup> single-resonance, variable-temperature in-situ probe. Spectra were taken

(19) Murakami, Y.; Inomata, M.; Miyamoto, A.; Mori, K. *Stud. Surf. Sci. Catal.* **1981**, *7*, 1344.

(20) Krishna, K. R.; Bell, A. T. *J. Catal.* **1991**, *130*, 597.

(21) Went, M. S. Ph.D. Thesis, University of California, Berkeley, 1991.

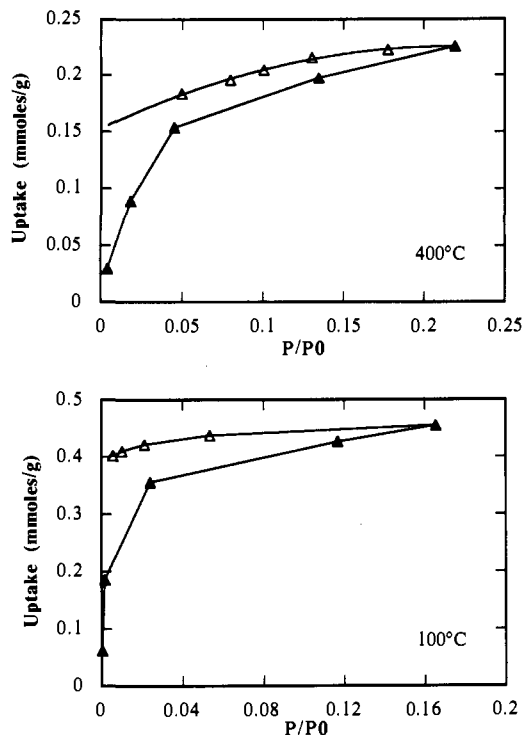


**Figure 1.** Ammonia uptake curves on 3.0 wt %  $V_2O_5/TiO_2$  at 400 °C (top) and 100 °C (bottom). Closed triangles are adsorption curves, and open triangles are desorption curves.

at room temperature, 200 K, and 100 K. Resonance positions are referenced to that of the protons in acetone at room temperature with the usual IUPAC convention, where positive numbers indicate increasing frequency. Ninety-degree pulse lengths were 3.5  $\mu$ s. Repetition delays between 2 and 10 s were used, and the number of averages varied from 400 to 16 000, with cosubtraction of alternating interferograms (FIDs).

The multiple-quantum experiments<sup>22,23</sup> were conducted such that only even-order coherences were allowed to develop. A standard eight-pulse cycle was used to create the average Hamiltonian  $H = \frac{1}{3}(H_{yy} - H_{xx})$  in the preparation period. The total cycle time was 93.6  $\mu$ s. The number of cycles was varied to yield total preparation times of up to 748.8  $\mu$ s. In the mixing period, the same sequence was used with all pulses phase-shifted by  $\pi/2$ . The delay between mixing and detection was 1 ms. Detection was accomplished with a single  $90^\circ$  pulse. The preparation-period pulse phases were cycled between 0 and  $\pi$  in alternate experiments and the time signals cosubtracted to reduce the unwanted<sup>22</sup> odd-order coherences. In addition, the detection pulse was phase-cycled between 0 and  $\pi$ , and the time signals were cosubtracted to reduce noise in the free-induction decay due to receiver ringdown.

In order to accomplish multiple-quantum spin counting, the phases of the preparation-period pulses were incremented from 0 to  $2\pi$ , thus separating coherence orders. For each phase, a magnitude was obtained as  $\sum (R_i^2 + I_i^2)^{1/2}$ , where  $R_i$  is the value of the real data point and  $I_i$  the value of the imaginary point and the sum is over the first 10 data points. The magnitude array was Fourier-transformed to yield an array of intensities corresponding to the coherence orders, or "stick spectra", with the number of resolvable orders equal<sup>23,24</sup> to half the number of increments. Thirty-two increments were used to give even orders from 2 to 16. The stick spectra were then baseline-corrected by subtraction of the rms value of the intensity of the odd-order coherences, which ideally should be zero. In order to observe two-quantum line shapes, the preparation-period pulse phases were incremented through many cycles of  $2\pi$  as the evolution period was also incremented according to the method<sup>25</sup> of time-proportional phase incrementation. Fourier transformation of the magnitude array yielded a frequency spectrum for each order, with the orders separated as before with a frequency bandwidth of  $\Delta\omega = \Delta\phi/\Delta t_1$ ,

(22) Baum, J.; Munowitz, M.; Garroway, A. N.; Pines, A. *J. Chem. Phys.* **1985**, *83*, 2015.

(23) Baum, J.; Gleason, K. K.; Pines, A.; Garroway, A. N.; Reimer, J. A. *Phys. Rev. Lett.* **1986**, *56*, 1377.

(24) Shykind, D. N.; Baum, J.; Liu, S.-B.; Pines, A. *J. Magn. Reson.* **1988**, *76*, 149.

(25) Bodenhausen, G.; Vold, R. L.; Vold, R. R. *J. Magn. Reson.* **1980**, *37*, 93.

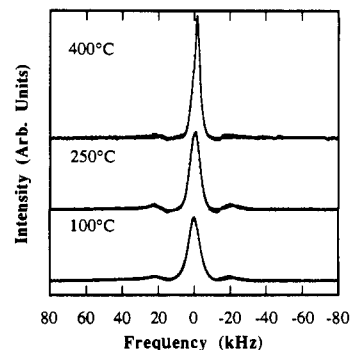


**Figure 2.** Room-temperature proton NMR spectra of  $NH_3$  adsorbed on  $TiO_2$  at 100, 250, and 400 °C along with least-squares fits to the theoretical line shapes (solid lines).

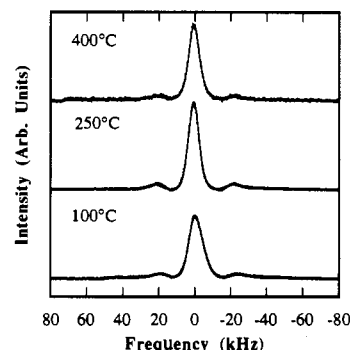


**Figure 3.** Room-temperature proton NMR spectra of  $NH_3$  adsorbed on 1.3 wt %  $V_2O_5/TiO_2$  at 100, 250, and 400 °C along with least-squares fits to the theoretical line shapes (solid lines).

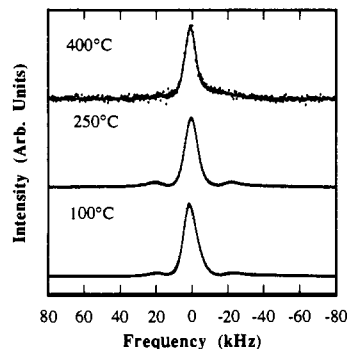


**Figure 4.** Room-temperature proton NMR spectra of  $NH_3$  adsorbed on 3.0 wt %  $V_2O_5/TiO_2$  at 100, 250, and 400 °C along with least-squares fits to the theoretical line shapes (solid lines).

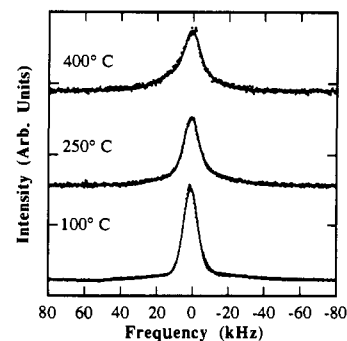


**Figure 5.** Room-temperature proton NMR spectra of  $NH_3$  adsorbed on 6.1 wt %  $V_2O_5/TiO_2$  at 100, 250, and 400 °C along with least-squares fits to the theoretical line shapes (solid lines).

where  $\Delta\phi$  is the phase increment and  $\Delta t_1$  the evolution period increment. The phase increment was  $2\pi/16$ , and  $\Delta t_1$  was 0.5  $\mu$ s, giving a bandwidth of 125 kHz. Thirty-two cycles of  $2\pi$  were used, for a total of 1024 points, or 64 points per order. Repetition delays of 1 or 2 s were used, and

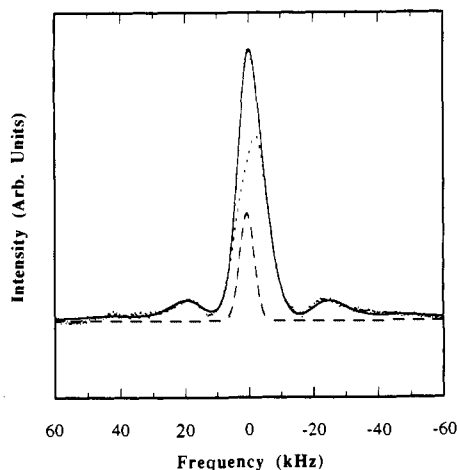


**Figure 6.** Proton NMR spectrum of  $\text{NH}_3$  adsorbed on 1.3 wt %  $\text{V}_2\text{O}_5/\text{TiO}_2$  at 100 °C along with the best fit to the theoretical line shape (solid line) and its individual components: dipolar triplet powder pattern (short dashes) and narrow Gaussian component (long dashes).

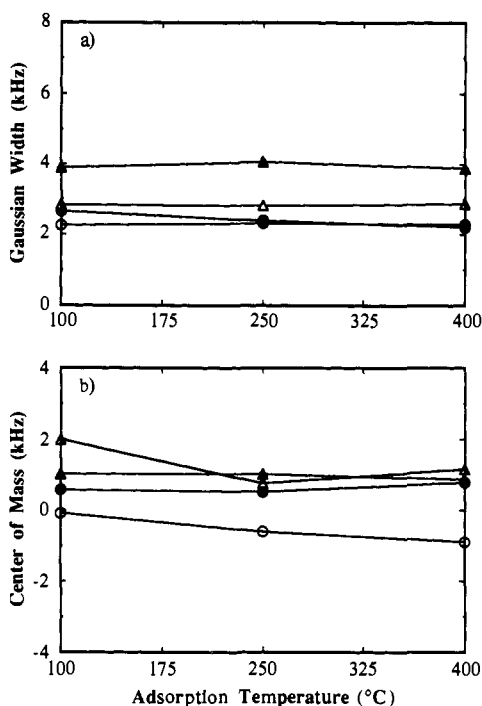


**Figure 7.** Parameters of narrow Gaussian components of proton line shapes for  $\text{NH}_3$  on  $\text{TiO}_2$  (open circles), 1.3 wt %  $\text{V}_2\text{O}_5/\text{TiO}_2$  (solid circles), 3.0 wt %  $\text{V}_2\text{O}_5/\text{TiO}_2$  (open triangles), and 6.1 wt %  $\text{V}_2\text{O}_5/\text{TiO}_2$  (solid triangles): (a) Gaussian width (square root of the second moment); (b) center of mass. For calcined samples prior to ammonia adsorption, Gaussian widths were 1.73, 2.32, 2.98, and 3.44 kHz and centers of mass were 2.03, 1.19, 2.25, and 1.94 kHz, respectively.

100–2400 signal averages<sup>26</sup> were taken for each spectrum.

In-situ deuteron NMR data were taken on a home-built spectrometer operating at frequency of 27.8 MHz using a solid echo ( $90^\circ_x - \tau - 90^\circ_y - \tau$ ) pulse sequence. Three- $\mu\text{s}$  pulses were used where the  $90^\circ$  pulse lengths were determined to be 4.5  $\mu\text{s}$  and the delay time  $\tau$  was 100- $\mu\text{s}$ . Spectra were corrected<sup>27</sup> for distortion due to finite pulse lengths.

## Results

Figures 2–5 show the proton spectra of ammonia adsorbed at 100, 250, and 400 °C on the  $\text{TiO}_2$  and the 1.3, 3.0, and 6.1 wt % samples. Shown along with the data are the least-squares fits to theoretical line shapes, arrived at using a nonlinear Newton–

(26) More averages were needed for longer preparation periods, where pulse imperfections and phase errors could accumulate over many cycles and multiple-quantum intensities were dissipated into higher orders.

(27) Bloom, M.; Davis, J. H.; Valic, M. I. *Can. J. Phys.* **1980**, *58*, 1510.

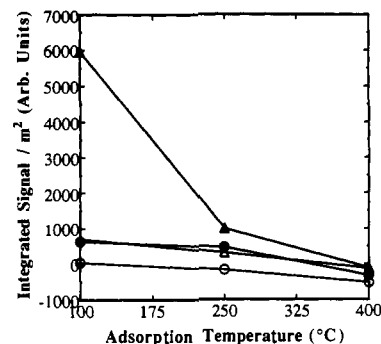


**Figure 8.** Residual areas, in arbitrary units, of narrow Gaussian components of proton line shapes per square meter of sample for  $\text{NH}_3$  on  $\text{TiO}_2$  (open circles), 1.3 wt %  $\text{V}_2\text{O}_5/\text{TiO}_2$  (solid circles), 3.0 wt %  $\text{V}_2\text{O}_5/\text{TiO}_2$  (open triangles), and 6.1 wt %  $\text{V}_2\text{O}_5/\text{TiO}_2$  (solid triangles). Areas of Gaussian line shapes of samples calcined prior to ammonia adsorption have been subtracted. They are 1170, 574, 320, and 318, respectively.

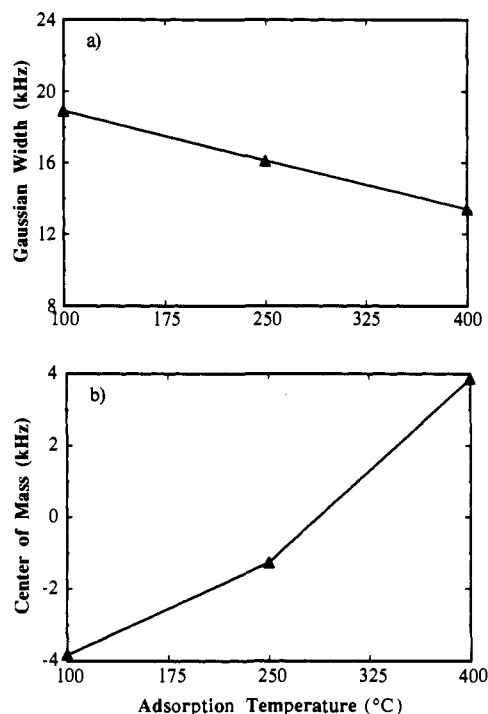


**Figure 9.** Parameters of the broad Gaussian component of the proton line shape for  $\text{NH}_3$  on 6.1 wt %  $\text{V}_2\text{O}_5/\text{TiO}_2$ : (a) Gaussian width (square root of the second moment); (b) center of mass.

Raphson algorithm which includes, a priori, the effects of left-shifting of data sets (a manifestation of which is apparent phase errors in the data). A table of all parameters determined<sup>21</sup> from the fits is available. On the titania and 1.3 wt % samples at all adsorption temperatures and on the 3.0 wt % sample after adsorption at 100 and 250 °C, the theoretical line shapes are a combination of a “narrow” Gaussian and a dipolar triplet powder pattern<sup>28</sup> with a splitting between outer singularities of 39.0–42.5 kHz. Figure 6 shows a representative decomposition of this theoretical line shape for ammonia adsorption at 100 °C on the 1.3 wt % sample. On the 3.0 wt % sample after adsorption at 400 °C and on the 6.1 wt % sample at all adsorption temperatures, the theoretical line shapes are composed of a narrow Gaussian and a broad Gaussian. Figures 7 and 8 summarize parameters of the narrow-Gaussian resonance. Figure 9 summarizes the parameters of the broad-Gaussian resonance. The assignment of these line shapes and their significance will be discussed below.

After completion of a set of experiments at one adsorption temperature, each sample was exposed to air at room temperature

(28) Andrew, E. R.; Bersohn, R. *J. Chem. Phys.* **1950**, *18*, 159.

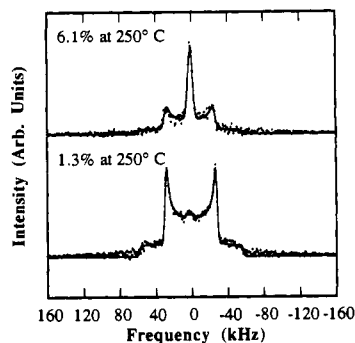


**Figure 10.** Deuteron NMR spectra for  $\text{ND}_3$  adsorbed on 6.1 wt %  $\text{V}_2\text{O}_5/\text{TiO}_2$  at 250 °C (top) and on 1.3 wt %  $\text{V}_2\text{O}_5/\text{TiO}_2$  at 250 °C (bottom), along with least-squares fits to the theoretical line shapes (solid lines).

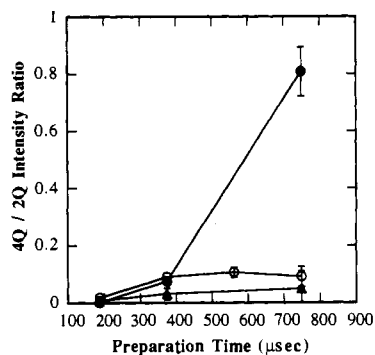


**Figure 11.** Relative four- to two-quantum coherence intensities as a function of total preparation time from multiple-quantum spin-counting experiments for  $\text{NH}_3$  adsorbed at 100 °C on  $\text{TiO}_2$  (open circles), 3.0 wt %  $\text{V}_2\text{O}_5/\text{TiO}_2$  (closed circles), and 6.1 wt %  $\text{V}_2\text{O}_5/\text{TiO}_2$  (triangles). Error bars represent the intensity of the three-quantum coherence.

and the proton spectrum then recorded. In all cases, a narrow Lorentzian line shape of much greater intensity than that of the adsorbed ammonia was observed, indicating a large uptake of ambient water.

Deuteron NMR spectra were taken after  $\text{ND}_3$  was adsorbed *statically* at saturation coverage ( $>80$  Torr) at 250 °C on the 1.3 and 6.1 wt % samples. The resulting spectra are shown in Figure 10, along with the least-squares fits to superpositions of quadrupolar doublets,<sup>29</sup> with splittings between singularities of 58.2 and 57.4 kHz for the 1.3 and 6.1 wt % samples, respectively, and narrow-Gaussian components. No signal was observed in a background spectrum that was taken after calcining in oxygen a 1.3 wt % sample that had been saturated previously with  $\text{D}_2\text{O}$ .

To probe further the molecular structure of the adsorbates, multiple-quantum spin counting was employed. Figure 11 shows the ratio of the four-quantum intensity to the two-quantum intensity for  $\text{NH}_3$  adsorbed at 100 °C on the 3.0 and 6.1 wt %  $\text{V}_2\text{O}_5/\text{TiO}_2$  samples, as well as on pristine  $\text{TiO}_2$ . Multiple-quantum coherences of order 6 or higher were not detected above the noise level for any of the catalyst samples. In contrast, spin-counting experiments done on hexamethylbenzene, a common standard, show the behavior expected<sup>22</sup> of an infinite system of coupled spins. Coherence orders of 2, 4, and 6 were observed for 187.2  $\mu\text{s}$  of preparation time, and up to 14 coherences (the highest detectable order) were observed above the noise level for the

(29) This splitting is dominated by the quadrupolar interaction of the deuteron (spin 1) nuclei in the presence of electric field gradients along the N–D bonds. Observation of spin 1 line shapes dates back to the early days of magnetic resonance. See, for example ref 34 or: Schumaker, R. *Magnetic Resonance*; W. A. Benjamin, Inc.: New York, 1970. For an early explanation of the solid echo sequence used to obtain our deuterium data, see: Davis, J. H.; Jeffrey, K. R.; Bloom, M.; Talic, M. I.; Higgs, T. P. *Chem. Phys. Lett.* **1976**, *42*, 390.

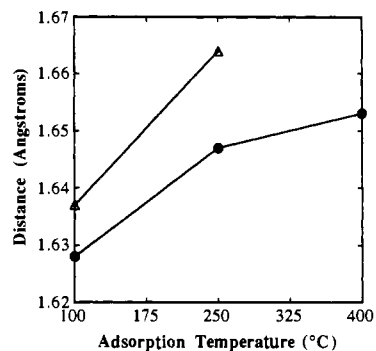


**Figure 12.** Proton–proton distances in  $\text{NH}_3$  adsorbed on 1.3 wt %  $\text{V}_2\text{O}_5/\text{TiO}_2$  (solid circles) and 3.0 wt %  $\text{V}_2\text{O}_5/\text{TiO}_2$  (open triangles) as determined from fits to theoretical line shapes. For gas-phase ammonia, the distance is 1.628 Å.

longest preparation times. The experimental protocol for observing multiple-quantum intensities was therefore appropriate.

### Discussion

The magnetic resonance data presented above identify four separate molecular structures after ammonia adsorption on the catalyst surfaces. They are (i) intact, coordinated, and rapidly rotating ammonia molecules, (ii)  $\text{NH}_x$  decomposition products, (iii) ammonium ( $\text{NH}_4^+$ ) ions, and (iv) surface hydroxyl groups. The assignments of the various resonances are discussed below. The distribution of these structures as functions of both surface composition and adsorption temperature is discussed within the context of adsorption sites.

**Intact Ammonia.** The powder line shape expected<sup>28</sup> from intact ammonia is a triplet resulting from the homonuclear dipolar interaction. The splitting between the singularities is 83.2 kHz for solid  $\text{NH}_3$  and is inversely proportional to the cube of the proton–proton distance. Rotation about the  $C_3$  axis that is rapid on the NMR time scale reduces the splitting by a factor of  $1/2$  to 41.6 kHz. Rotating, adsorbed ammonia has been observed previously<sup>30</sup> by proton NMR spectroscopy of molybdenum nitride surfaces. The proton spectra taken after adsorption of ammonia on the lower weight loading samples fit well to this theoretical line shape, convoluted with a Gaussian, with splittings ranging between 39.0 and 42.5 kHz. The powder pattern is thus assigned to intact, rotating  $\text{NH}_3$  chemisorbed on the surface. The Gaussian broadening on the triplet ranges from 0.8 to 4.2 kHz and derives from heteronuclear  $^{14}\text{N}$ – $^1\text{H}$  dipolar interactions, site inhomogeneity, field inhomogeneity, and paramagnetic susceptibility broadening from reduced vanadia species on the catalyst surface.

Deuteron results confirm this assignment to intact, rotating ammonia. The observed quadrupolar doublet splittings correspond<sup>31</sup> well to the 54 kHz value observed<sup>32</sup> previously for the splitting in the line shape of rapidly rotating adsorbed  $\text{ND}_3$ .

On the basis of the above assignments, it is concluded that strongly bound, intact, and rapidly rotating ammonia molecules are present on the 0, 1.3, and 3.0 wt %  $\text{V}_2\text{O}_5/\text{TiO}_2$  samples. From the theoretical line shapes that best fit the data, proton–proton distances were determined. Figure 12 is a plot of these distances as a function of adsorption temperature for the 1.3 and 3.0 wt % samples. The distance increases both as the adsorption temperature increases and as the weight loading increases. Two possible interpretations are (i) that the N–H bond is lengthening and (ii) that the H–N–H angle is increasing. On the basis of Raman spectroscopy results,<sup>18</sup> which indicate a constant N–H

(30) Haddix, G. W.; Jones, D. H.; Bell, A. T.; Reimer, J. A. *J. Catal.* **1988**, *112*, 556.

(31) Our failure to observe intact  $\text{NH}_3$  in the proton spectra of the 6.1 wt % sample at 250 °C, while observing it in the deuteron spectra, is explained by noting that the proton results are obscured by large broadening and low intensity vis-à-vis other spectral features. Furthermore, the discrepancy in sample preparation conditions—static vs flowing adsorptions—may have some effect.

(32) Majors, P. D.; Raidy, T. E.; Ellis, P. D. *J. Am. Chem. Soc.* **1986**, *108*, 8123.

bond length under identical conditions on these same samples, case i is ruled out. Assuming case ii to be true, the change in H-H distance obtained from our NMR measurements can be directly translated into a change in H-N-H bond angle from 107.3° (the value for gas-phase ammonia) to ~111°. Assuming a simple potential function for the ammonia molecule,<sup>33</sup> this change in ammonia bond angle costs approximately 36 cm<sup>-1</sup> of energy. This destabilization of the ammonia molecule is presumed to be concomitant with increasing strength of the ammonia-surface bond, as well as with increased reactivity of the ammonia adsorbate. This picture is consistent with the TPD results,<sup>18</sup> which suggest that intact ammonia is more strongly bound on the 3.0 wt % than on the 1.3 wt % sample and is more likely to decompose. Observation of little or no intact ammonia in the proton NMR spectra of the 6.1 wt % sample is also consistent with the TPD results, which show that intact NH<sub>3</sub> desorbs at a significantly lower temperature and that the fraction of dissociated products is greater on this sample. Ammonia adsorption on pristine TiO<sub>2</sub>, however, yields an H-H distance that is roughly constant with adsorption temperature and is slightly smaller than that observed on the supported samples. On all samples, the amount of adsorbed, intact NH<sub>3</sub> decreases as the adsorption temperature is increased.

**Ammonia Decomposition Products.** At the point where intact ammonia is no longer observed on the higher weight loading samples, a broad Gaussian resonance is observed. This broad Gaussian is shifted relative to the triplet powder pattern; on the 3.0 wt % sample, the center of mass of the broad Gaussian observed after ammonia adsorption at 400 °C is 4.6 kHz, whereas the centers of mass of the powder patterns are -1.6 and 0.3 kHz after 100 and 250 °C ammonia adsorptions, respectively. Figure 9b shows the center of mass of the broad Gaussian peak as a function of adsorption temperature for the 6.1 wt % sample. The resonance shifts to higher frequency as the adsorption temperature is increased. These observations suggest that the broad Gaussian is associated with a new stable species, most likely a decomposition product, present on the surface under the conditions of higher adsorption temperature and higher weight loading.

In contrast to the other surface resonances, the first moment of the broad Gaussian depends strongly (up to 20 ppm shift) upon the oxidation state (i.e. ammonia adsorption temperature) of the catalyst. Indeed, on the 6.1 wt % sample, a significant shift and broadening of the broad Gaussian was observed when the NMR sample temperature was reduced. This is consistent with a paramagnetic effect<sup>36</sup> or temperature-dependent contact shift. Combining these observations, we suggest that the moiety associated with this broad Gaussian resonance is in close proximity to reduced or reducible vanadium atoms. Furthermore, large paramagnetic susceptibility broadening may explain the lack of structural features in the line shape.

Because the line shapes show no structure, a moment analysis was used to help identify the species responsible for the broad Gaussian components. The Gaussian second moments, shown in Figure 9a, are 18.9, 16.1, and 13.4 kHz on the 6.1 wt % sample at adsorption temperatures of 100, 250, and 400 °C, respectively. These widths can be compared to those calculated using the Van Vleck equation,<sup>34</sup> as shown in Table II. Gaseous ammonia and methylamine geometries<sup>35</sup> were used for calculations pertaining to NH<sub>3</sub> and NH<sub>2</sub> species, respectively. Non-dipolar broadening was conservatively estimated at 3 kHz from the widths of the

Table II. Second-Moment Calculations

species	$M_2^{1/2}$ (kHz)			residual	tot.
	H-H	N-H <sup>a</sup>	V-X-H <sup>a,b</sup>		
rigid NH <sub>3</sub>	26.5	(6.2)	(6.1) (2.5 <sup>c</sup> )	3.0	28.0 24.5
rotating NH <sub>3</sub>	13.2	1.8		3.0	13.7
rigid NH <sub>2</sub>	19.0	(6.1)	(6.1) (2.5 <sup>c</sup> )	3.0	21.0 20.3
rotating NH <sub>2</sub>	9.5	0.3		3.0	9.9
rigid NH		(6.1)	(6.1) (2.5 <sup>c</sup> )	3.0	9.1 7.2
rigid VOH <sup>d</sup>			6.1	3.0	6.8
rotating VOH <sup>d</sup>			2.5	3.0	3.9

<sup>a</sup>Number in parentheses indicates moments calculated as if N and/or V were in nuclear Zeeman states. The actual nuclear states are described by the quadrupolar interaction and, thus the moments are approximately 40% larger. <sup>b</sup>X = O or N; V-X distance taken to be that of V-O in crystalline V<sub>2</sub>O<sub>5</sub>. <sup>c</sup>Calculated by assuming rigid N-H bonds but free rotation about the V-X bond. <sup>d</sup>O-H bond length and angle taken to be identical to those of water.

background peaks emanating from hydroxyl groups on the calcined samples. The sum of the heteronuclear (N-H) and homonuclear (H-H) dipolar contributions to the square root of the second moment,  $M_2^{1/2}$ , of a rigid NH<sub>2</sub> group with bonding as in methylamine is expected to be 21 kHz. Rapid rotation would reduce this to 10 kHz.  $M_2^{1/2}$  for an isolated NH group is expected to be 7-9 kHz. The observed values are all larger than that expected for NH-type moieties but slightly less than that expected for a rigid NH<sub>2</sub> group. Because motion will only reduce the second moment, we tentatively assign<sup>36</sup> the broad peak to NH<sub>2</sub> groups that are experiencing varying degrees of hindered motion. This NH<sub>2</sub> decomposition product is most prevalent in catalysts with large vanadia loadings. We conclude that one role of the concentrated vanadia is to facilitate decomposition of the NH<sub>3</sub>.

Some infrared spectroscopy studies<sup>11,15</sup> support the existence of surface NH<sub>2</sub> groups on titania-supported vanadia. Furthermore, indirect evidence for their existence is supplied<sup>37,38</sup> by <sup>15</sup>N isotopic tracer studies. Others<sup>37,39,40</sup> have postulated the possible catalytic importance of NH<sub>2</sub>.

It was hoped that the two-quantum line shapes might contain resolved features from NH<sub>2</sub> groups, thus providing useful structural information, analogous to prevent work<sup>41</sup> in which resolved multiple-quantum line shape features were obtained for benzene oriented in a liquid crystal. Also, comparison of the second moments of the two-quantum line shapes with predictions based on the size of the effective spin system<sup>42</sup> might have yielded information that could have been used to help establish with certainty the presence (or absence) of two-spin systems. However, the two-quantum second moments on the two vanadia/titania samples are equal, and that for adsorption on pure titania is slightly larger. Qualitatively, the two-quantum line shapes appear similar for all three samples, and none show features that could be useful in structure determination. This is not too surprising since the two-quantum line shape may contain transitions from NH<sub>3</sub> and NH<sub>4</sub>, as well as NH<sub>2</sub>, moieties.

**Ammonium Ions and Surface Hydroxyls.** The narrow Gaussian is observed on all weight loading samples at all adsorption temperatures, with roughly the same features in each case. The Gaussian second moments range from 2.3 kHz on the TiO<sub>2</sub> sample to 3.9 kHz on the 6.1 wt % sample, as shown in Figure 7a. The general trend is for an increase in the width as weight loading is increased. The center of mass, shown in Figure 7b, shifts slightly

(33) Coon, J. B.; Naugle, N. W.; McKenzie, R. D. *J. Mol. Spectrosc.* **1966**, *20*, 107.

(34) Abragam, A. *The Principles of Nuclear Magnetism*; Oxford University Press: Oxford, U.K., 1961.

(35) *Handbook of Chemistry and Physics*; CRC Press: Boca Raton, FL, 1985.

(36) Static ND<sub>x</sub> bonds were not observed in any of the deuteron experiments, in seeming contradiction to the proton data. Our deuteron experiments, however, were performed after static adsorption of ND<sub>3</sub> and were not done on samples in which NH<sub>2</sub> fragments dominate (e.g., 6 wt % vanadia, 400 °C adsorption temperature). Furthermore, rotating ND<sub>2</sub> would give a splitting of 10-15 kHz, which would be especially hard to resolve, given the residual sources of broadening. Also, the extreme breadth of the quadrupolar doublet in static ND systems (>200 kHz) limits our sensitivity to this species.

(37) Janssen, F. J. J. G.; van den Kerkhof, F. M. G.; Bosch, H.; Ross, J. R. *H. J. Phys. Chem.* **1987**, *91*, 6633.

(38) Miyamoto, A.; Kobayashi, K.; Inomata, M.; Murakami, Y. *J. Phys. Chem.* **1982**, *86*, 2945.

(39) Janssen, F. J. J. G.; van den Kerkhof, F. M. G.; Bosch, H.; Ross, J. R. *H. J. Phys. Chem.* **1987**, *91*, 5221.

(40) Farber, M.; Harris, S. P. *J. Phys. Chem.* **1984**, *88*, 680.

(41) (a) Warren, W. S.; Sinton, S.; Weitekamp, D. P.; Pines, A. *Phys. Rev. Lett.* **1979**, *43*, 1791. (b) Warren, W. S.; Pines, A. *J. Chem. Phys.* **1981**, *74*, 2808.

(42) Yen, Y. S. Ph.D. Thesis, University of California, Berkeley, 1982.

to higher frequency as weight loading is increased. Possible assignments of this peak include residual hydroxyl groups from incomplete dehydroxylation of the surface in the pretreatment of the samples, hydroxyl groups or isolated NH groups formed from dissociative adsorption of NH<sub>3</sub>, or ammonium ions.

The anticipated width of a signal emanating from an isolated NH group is significantly larger than 3.9 kHz, as shown in Table II, and therefore this assignment can be ruled out. The spectra of residual surface hydroxyls were obtained from freshly calcined samples, each of which is well fit to a Gaussian with width ranging from 1.7 kHz in the case of TiO<sub>2</sub> to 3.4 kHz for the 6.1 wt % sample. The centers of mass of the Gaussian peaks observed on the calcined samples, indicated in the caption of Figure 7, are nearly the same as those of the narrow Gaussians observed on the NH<sub>3</sub>-treated samples. On the basis of this comparison alone, assignment to surface hydroxyls is plausible. Figure 8 shows the relative integrated areas of the narrow Gaussian after subtraction of the areas of the peaks emanating from the calcined samples, for the three adsorption temperatures on all four samples. In the spectra of the titania samples that have been exposed to ammonia, the narrow Gaussian areas are equal to or less than the corresponding area from the calcined sample, indicating that the narrow resonance indeed can be attributed to the surface hydroxyl groups. On the vanadia-containing samples, however, it is apparent that at 100 and 250 °C more intensity in the narrow Gaussian is observed in the presence of adsorbed NH<sub>3</sub> than can be accounted for by residual hydroxyls. It is concluded, therefore, that at these temperatures the narrow Gaussian derives from protons associated with ammonium ions (NH<sub>4</sub><sup>+</sup>).

This assignment is consistent with the deuteron spectra, which show the narrow resonance anticipated from ND<sub>4</sub><sup>+</sup> ions tumbling rapidly at room temperature, as observed previously<sup>32</sup> for ND<sub>4</sub><sup>+</sup> ions on oxide surfaces. In both the proton and deuteron spectra, the intensity of the NH<sub>4</sub><sup>+</sup> peak, expressed per square meter of catalyst surface, is greatest on the 6.1 wt % sample. Taking into account the surface structure,<sup>7</sup> it appears that ammonium ions form predominantly on polymeric vanadia species.

The deuteron NMR spectra do not indicate the presence of deuterioxy groups formed from dissociative adsorption of ND<sub>3</sub>. The line shape of OD groups would<sup>32</sup> be a doublet powder pattern with a large splitting of 210 kHz. Even with diminished sensitivity to such broad lines, it is concluded that *stable* OD groups are not formed from dissociative adsorption of ND<sub>3</sub>.

While no *stable* hydroxyls are formed from ammonia decomposition, it is possible that hydroxyls are formed which subsequently react very quickly in the catalytic environment. The intensity of the narrow Gaussian assigned to NH<sub>4</sub><sup>+</sup> after ammonia adsorption at 100 °C is approximately twice the intensity of the hydroxyl resonance on the calcined 1.3 wt % sample. On this sample, then, the ammonium ion could form from preexisting hydroxyl groups. On the 6.1 wt % sample, however, the intensity of the NH<sub>4</sub><sup>+</sup> peak after adsorption at 100 °C is approximately 30 times greater than the intensity of the hydroxyl peak on the calcined sample. Additional OH groups acting as Bronsted acid sites strong enough to coordinate the ammonium ion must be formed. Because no *stable* OD groups are observed after adsorption of ND<sub>3</sub>, we infer that hydroxyls (or deuterioxy groups) are formed from dissociative adsorption of NH<sub>3</sub> (or ND<sub>3</sub>) but that, in the presence of NH<sub>3</sub>, these hydroxyls react very quickly to form the more stable ammonium ions. Furthermore, this occurs on vanadia and not on titania. A recent IR study has shown<sup>11</sup> the existence of a hydroxyl band assigned to VOH on titania-supported vanadia following adsorption of water and its disappearance following subsequent adsorption of ammonia. This provides additional evidence that VOH groups form and are easily converted to VO-NH<sub>4</sub><sup>+</sup> in the presence of ammonia gas. The decrease in intensity of the NH<sub>4</sub><sup>+</sup> peak with increasing temperature implies that the ammonium ion is weakly bound and easily removed from the surface by heating, consistent with the IR studies discussed above.

After adsorption at 400 °C, the ammonium ions have been mostly removed and the narrow Gaussian represents the residual

hydroxyl groups. Figure 8 shows that fewer hydroxyls remain on the surface at 400 °C than were originally present on all four oxidized samples, indicating irreversible depletion of hydroxyls by ammonia reduction. This has been observed previously on titania<sup>10,43</sup> and on silica.<sup>12</sup> Additional hydroxyls on the surface dehydrate, with water being given off. This explanation is consistent with TPD results which show<sup>18</sup> two H<sub>2</sub>O peaks emanating from the vanadia-containing samples. The high-temperature peak, which also emanates from pristine TiO<sub>2</sub>, results from a reaction of the NH<sub>3</sub> to form H<sub>2</sub>O, and the low-temperature peak that is concomitant with NH<sub>3</sub> desorption arises from dehydration of the surface VOH species. Furthermore, oxygen-18 isotope studies<sup>39</sup> showed that water from dehydration of the surface evolves slowly relative to water formed from a reaction of NH<sub>3</sub>, NO, and O<sub>2</sub>, as oxygen from the gas phase is slowly exchanged into the surface. The lability of the surface oxygen was found<sup>39</sup> to be greatest on the monolayer V<sub>2</sub>O<sub>5</sub>/TiO<sub>2</sub> catalysts and greater at higher temperatures.

Low-temperature proton spectra were taken for all of the sample conditions described above. On all of the TiO<sub>2</sub> and the 1.3 and 3.0 wt % samples, no significant (greater than 10%) increases in line width of either the powder pattern or the narrow Gaussian were observed. This indicates that, at room temperature, rapid surface diffusional motion is unlikely and a freezing of rotational motion of the intact NH<sub>3</sub> does not occur.

Multiple-quantum spin-counting and line shape analysis experiments were done in anticipation of providing further confirmation of the identities of postulated adsorbed species on the catalytic surfaces. The results shown in Figure 11 indicate that four-quantum coherences exist at the longest preparation times examined on all samples. For the excitation Hamiltonian  $H = \frac{1}{3}(H_{yy} - H_{xx})$ , the existence of a four-quantum coherence is indicative of a spin system consisting of at least five coupled spins.<sup>44,45</sup> Therefore, it is concluded that groups of five or more correlated spins exist on the surfaces of the TiO<sub>2</sub> and the 3.0 and 6.1 wt % samples following ammonia adsorption at 100 °C. This suggests that couplings between various adsorbed species, such as surface hydroxyls and intact adsorbed ammonia, or within a single species, such as closely associated surface hydroxyl groups, occur. Further interpretation of these data is difficult. The spin-counting experiments did not provide independent confirmation of the identities of adsorbed species. Investigation of the dynamics of the growth of multiple-spin coherences was not a goal of this study, and data points were collected for only three or four preparation times for each sample. However, it is apparent that the dynamics are very different on the different samples. Furthermore, these differences appear at first to be inconsistent with the relative proton concentrations obtained from the single-quantum spectra. Specifically, the four-quantum coherence develops more rapidly on the 3.0 wt % sample, which has the lowest total proton concentration of the three. Given that they are reliable, reconciliation of these data is possible if one assumes that clustering (of some combination of adsorbed ammonia, ammonium ions, and hydroxyl groups) occurs on this sample. Again, 6- or higher-order coherences (expected from groups of six or more correlated spins), if present on these samples, were obscured in the noise of the data.

We remain cautious, however, in our interpretation of the results of the multiple-quantum spin-counting experiments, given the large magnitude of error. Sensitivity was discovered to be a large limitation in performing multiple-quantum experiments for NH<sub>3</sub> adsorbed on these catalysts. In particular, the optimization of experimental parameters, such as the preparation pulse sequence cycle time and the total preparation-period time, which is apparently necessary to obtain resolution of line shape features, is impractical when one experiment requires several days of signal averaging. It was discovered, not surprisingly, that extremely

(43) Primet, M.; Pichat, P.; Mathieu, M. *J. Phys. Chem.* 1971, 75, 75.

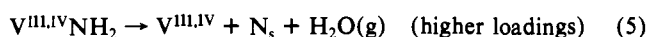
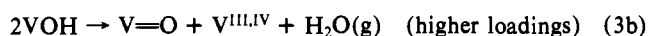
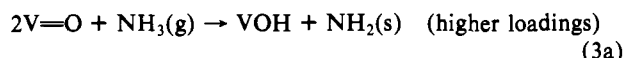
(44) Munowitz, M. *Coherence and NMR*; Wiley: New York, 1988.

(45) Munowitz, M.; Pines, A.; Mehring, M. *J. Chem. Phys.* 1987, 86, 3172.

steady and constant probe tuning, and therefore highly accurate pulses, are essential. As noted already, the two-quantum line shapes that we obtained did not provide us with any additional information with which to identify adsorbed species.

### Conclusions

NMR spectroscopic techniques have allowed direct quantitative observation of coordinatively adsorbed ammonia,  $\text{NH}_4^+$  ions, a decomposed species assigned to  $\text{NH}_2$ , and surface hydroxyls. The observed distribution of these species as a function of adsorption temperature and catalyst compositions suggests the following scheme for the adsorption and decomposition of ammonia on these catalysts:



Reactions 2a and 2b represent the coordinative adsorption of ammonia to the Lewis acid sites of the vanadia and the titania. Reaction 3a represents the decomposition of  $\text{NH}_3$  on the higher weight loading samples. Reaction 4, the formation of ammonium ions, is a fast reaction that occurs on all vanadia-containing samples where surface hydroxyls are present, but in greater proportion on the higher weight loading samples where the ammonia decomposition makes available additional hydroxyl groups. Reactions 3b and 3c represent the dehydration and reduction of the surface and most likely account for the low-temperature water desorption peak that is concomitant with the ammonia desorption (reaction 4) on the higher weight loading samples, as well as the reduction of vanadium atoms to the +3 or +4 state. Reaction 5 is the formation of surface N atoms that can lead to  $\text{N}_2$  or other

dissociated nitrogen products; it also represents additional water formation from the decomposed ammonia and could explain the second high-temperature water peak in the TPD<sup>18</sup> of the 3.0 and 6.1 wt % samples, which coincides with the evolution of nitrogen products.

If extrapolation of the observations of adsorbed ammonia to conditions where  $\text{NO}_x$  and oxygen are also present is possible, it is surmised that ammonium ions are not responsible for the majority of the catalytic activity, as they are easily removed by heating to temperatures below those where the activity reaches a maximum. In addition, observation of rapidly rotating ammonia, under all conditions where intact ammonia is observed, strongly suggests that any long-lived activated complex involving adsorbed ammonia fixed to more than one site on the surface (i.e. H-bonded to several neighboring oxygen atoms) is unlikely. These results put an upper limit on the lifetime of such species (as has been proposed in the Eley-Rideal mechanism<sup>2,38,39</sup>) of about one measured rotational period of the adsorbed ammonia, which is no greater than  $\sim 10 \mu\text{s}$  at room temperature.

The results presented here and elsewhere suggest that dissociative adsorption of ammonia occurs predominantly on polymeric vanadia species where surface VO bonds are in close proximity to one another and results in increased activity but decreased selectivity toward nitrogen in the selective catalytic reduction reaction. Indeed, reduced sites are also found to be active for the SCR mechanism.<sup>3</sup> A coordinated  $\text{NH}_2\text{NO}$  species reacting to form  $\text{N}_2 + \text{H}_2\text{O}$ , as proposed on the basis of mass spectrometric studies,<sup>40</sup> may be a key intermediate.

**Acknowledgment.** We wish to acknowledge technical discussions with Professor Alexis T. Bell and his research group. We also wish to thank Heather Rumsey for assistance with the sample preparation and surface area measurements and Phil Armstrong for assistance with the deuterium NMR experiments. This work was supported by the Director, Office of Energy Research, Office of Basic Energy Sciences, Materials Sciences Division of the U.S. Department of Energy, under Contract DEACO3-76SF00098.

**Registry No.**  $\text{V}_2\text{O}_5$ , 1314-62-1;  $\text{TiO}_2$ , 13463-67-7; ammonia, 7664-41-7.

## Glass Formation and Structure in Non-Oxide Chalcogenide Systems. The Short Range Order of $\text{Ag}_2\text{S}-\text{P}_2\text{S}_5$ Glasses Studied by $^{31}\text{P}$ MAS-NMR and Dipolar NMR Techniques

Zhengming Zhang, John H. Kennedy, and Hellmut Eckert\*

Contribution from the Department of Chemistry, University of California, Santa Barbara, California 93106. Received January 13, 1992

**Abstract:** Glass formation and the local structure of ionically conductive crystalline and glassy compositions in the  $(\text{Ag}_2\text{S})_x(\text{P}_2\text{S}_5)_{1-x}$  system have been investigated by  $^{31}\text{P}$  magic-angle spinning (MAS) and spin-echo NMR. Glass formation encompasses the compositional range  $0.5 \leq x \leq 0.67$ .  $^{31}\text{P}$  MAS and spin-echo NMR data reveal striking differences in the local structure of the glasses and their crystalline counterparts. This result reinforces previous findings in related pseudobinary chalcogenide systems. A detailed examination of the  $\text{Ag}_2\text{S}-\text{P}_2\text{S}_5$  phase diagram reveals seven stable crystalline pseudobinary compounds with stoichiometries  $\text{Ag}_3\text{PS}_3$ ,  $\text{Ag}_4\text{P}_2\text{S}_5$  (two crystallographic modifications),  $\text{Ag}_4\text{P}_2\text{S}_7$ ,  $\text{Ag}_7\text{P}_3\text{S}_{11}$ ,  $\text{Ag}_3\text{PS}_4$ , and  $\text{Ag}_7\text{PS}_6$ , respectively, plus an additional compound with yet uncertain stoichiometry. The  $^{31}\text{P}$ - $^{31}\text{P}$  dipole-dipole coupling present in P-P and P-S-P connectivities in these phases has been characterized by means of spin-diffusion measurements under MAS conditions. This technique appears particularly useful in the compositional and structural analysis of multicomponent phase mixtures as they arise from the crystallization of glasses.

### Introduction

The discovery of very high ionic conductivity in a new class of sulfide-based glasses has been one of the most significant developments in the field of solid electrolytes in the past few years.<sup>1-13</sup>

These glasses form by rapid quenching of melts containing  $\text{Li}_2\text{S}$ ,  $\text{LiI}$ , and stoichiometric group III-V sulfides, such as  $\text{B}_2\text{S}_3$ ,  $\text{SiS}_2$ ,

(1) Malugani, J. P.; Robert, G. *Solid State Ionics* 1980, 1, 519.